

Enzymatically Amplified Surface Plasmon Resonance Imaging Detection of DNA by Exonuclease III Digestion of DNA Microarrays

Hye Jin Lee, Yuan Li, Alastair W. Wark, and Robert M. Corn*

Department of Chemistry, University of California—Irvine, Irvine, California 92697

This paper describes a novel approach utilizing the enzyme exonuclease III in conjunction with 3'-terminated DNA microarrays for the amplified detection of single-stranded DNA (ssDNA) with surface plasmon resonance (SPR) imaging. When *ExoIII* and target DNA are simultaneously introduced to a 3'-terminated ssDNA microarray, hybridization adsorption of the target ssDNA leads to the direction-dependent *ExoIII* hydrolysis of probe ssDNA strands and the release of the intact target ssDNA back into the solution. Readsorption of the target ssDNA to another probe creates a repeated hydrolysis process that results over time in a significant negative change in SPR imaging signal. Experiments are presented that demonstrate the direction-dependent surface enzyme reaction of *ExoIII* with double-stranded DNA as well as this new enzymatically amplified SPR imaging process with a 16-mer target ssDNA detection limit of 10–100 pM. This is a 10^2 – 10^3 improvement on previously reported measurements of SPR imaging detection of ssDNA based solely on hybridization adsorption without enzymatic amplification.

DNA microarrays are a fast and inexpensive way to obtain sequence-specific nucleic acid information for gene analysis,^{1,2} viral identification,^{3,4} medical diagnostics,^{5,6} and many other biological applications.^{7,8} Sequence specificity is obtained by detection of the surface hybridization of target molecules from solution onto the various array elements. Fluorescence imaging is typically used to detect the hybridization adsorption of tagged DNA molecules

onto the array,^{9–13} and SPR imaging^{10,14–22} is an alternative, “label-free” refractive index method that can be used to detect the adsorption of untagged DNA and RNA molecules. Fluorescence imaging is often limited by background to a detection limit of 1 pM,^{9,10,12} and SPR imaging typically has a detection limit of 1–10 nM.^{10,14,21–23} Recently, we have demonstrated that this detection limit can be lowered to 1 fM by using the enzyme RNase H in conjunction with an RNA microarray for the enzymatic amplification of the SPR imaging signal.^{16,17} Despite the excellent sensitivity and selectivity of this method, it has the limitation of requiring an RNA microarray as compared to a DNA microarray. RNA microarrays^{16,17} are stable but not yet widely used since they require special handling to avoid enzymatic or chemical destruction. A question that immediately arises is, can we use an alternative enzymatic amplification system that will work with DNA microarrays?

In this paper, we explore the use of the enzyme exonuclease III (*ExoIII*) in conjunction with DNA microarrays for the enzymatically amplified detection of DNA. *ExoIII* exhibits 3' → 5' exodeoxyribonuclease activity, which involves specific binding to double-stranded DNA (dsDNA) followed by selective hydrolysis of one strand from the DNA duplex. The direction-dependent behavior of the *ExoIII* activity was investigated to demonstrate that an

* To whom correspondence should be addressed. E-mail: rcorn@uci.edu.

- (1) Gerion, D.; Chen, F.; Kannan, B.; Fu, A.; Parak, W. J.; Chen, D. J.; Majumdar, A.; Alivisatos, A. P. *Anal. Chem.* **2003**, *75*, 4766–4772.
- (2) Lockhart, D. J.; Winzeler, E. A. *Nature* **2000**, *405*, 827–836.
- (3) Chen, C. C.; Teng, L. J.; Kaiung, S.; Chang, T. C. *J. Clin. Microbiol.* **2005**, *43*, 1515–1521.
- (4) Lin, B.; Vora, G. J.; Thach, D.; Walter, E.; Metzgar, D.; Tibbetts, C.; Stenger, D. A. *J. Clin. Microbiol.* **2004**, *42*, 3232–3239.
- (5) Cobb, J. P.; Mindrinos, M. N.; Miller-Graziano, C.; Calvano, S. E.; Baker, H. V.; Xiao, W.; Laudanski, K.; Brownstein, B. H.; Elson, C. M.; Hayden, D. L.; Herndon, D. N.; Lowry, S. F.; Maier, R. V.; Schoenfeld, D. A.; Moldawer, L. L.; Davis, R. W.; Tompkins, R. G. *Proc. Natl. Acad. Sci. U. S. A.* **2005**, *102*, 4801–4806.
- (6) Young, R. A. *Cell* **2000**, *102*, 9–15.
- (7) Sergeev, N.; Distler, M.; Courtney, S.; Al-Khaldi, S. F.; Volokhov, D.; Chizhikov, V.; Rasooly, A. *Biosens. Bioelectron.* **2004**, *20*, 684–698.
- (8) Debouck, C.; Goodfellow, P. *Nat. Genet.* **1999**, *21*, 48–50.

- (9) Lehr, H.-P.; Reimann, M.; Brandenburg, A.; Sulz, G.; Klapproth, H. *Anal. Chem.* **2003**, *75*, 2414–2420.
- (10) Livache, T.; Maillart, E.; Lassalle, N.; Mailley, P.; Corso, B.; Guedon, P.; Roget, A.; Levy, Y. *J. Pharm. Biomed. Anal.* **2003**, *32*, 687–696.
- (11) Epstein, J. R.; Biran, I.; Walt, D. R. *Anal. Chim. Acta* **2002**, *469*, 3–36.
- (12) Zammattéo, N.; Jeanmart, L.; Hamels, S.; Courtois, S.; Louette, P.; Hevesi, L.; Remacle, J. *Anal. Biochem.* **2000**, *280*, 143–150.
- (13) van Hal, N. L. W.; Vorst, O.; van Houwelingen, A. M. M. L.; Kok, E. J.; Peijnenburg, A.; Aharoni, A.; van Tunen, A. J.; Keijer, J. *J. Biotechnol.* **2000**, *78*, 271–280.
- (14) Okumura, A.; Sato, Y.; Kyo, M.; Kawaguchi, H. *Anal. Biochem.* **2005**, *339*, 328–337.
- (15) Wilkop, T.; Wang, Z.; Cheng, Q. *Langmuir* **2004**, *20*, 11141–11148.
- (16) Goodrich, T. T.; Lee, H. J.; Corn, R. M. *J. Am. Chem. Soc.* **2004**, *126*, 4086–4087.
- (17) Goodrich, T. T.; Lee, H. J.; Corn, R. M. *Anal. Chem.* **2004**, *76*, 6173–6178.
- (18) Rella, R.; Spadavecchia, J.; Manera, M. G.; Siciliano, P.; Santino, A.; Mita, G. *Biosens. Bioelectron.* **2004**, *20*, 1140–1148.
- (19) Shumaker-Parry, J. S.; Campbell, C. T. *Anal. Chem.* **2004**, *76*, 907–917.
- (20) Kanda, V.; Kariuki, J. K.; Harrison, D. J.; McDermott, M. T. *Anal. Chem.* **2004**, *76*, 7257–7262.
- (21) Nelson, B. P.; Grimsrud, T. E.; Liles, M. R.; Goodman, R. M.; Corn, R. M. *Anal. Chem.* **2001**, *73*, 1–7.
- (22) Guedon, P.; Livache, T.; Martin, F.; Lesbre, F.; Roget, A.; Bidan, G.; Levy, Y. *Anal. Chem.* **2000**, *72*, 6003–6009.
- (23) Wark, A. W.; Lee, H. J.; Corn, R. M. *Anal. Chem.* **2005**, in print.

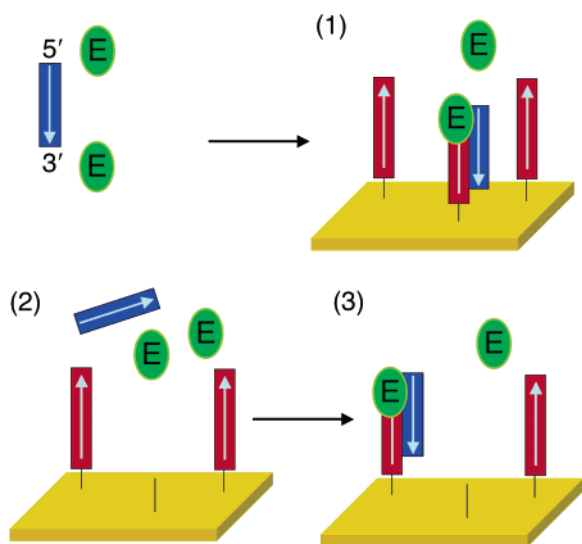


Figure 1. (a) Schematic representation of the surface *ExoIII* process for the amplification of SPR signal by selective removal of DNA probes from the dsDNA microarray. (1) An ssDNA array is exposed to a solution containing target DNA and *ExoIII*; the target DNA hybridizes to its complementary ssDNA array elements and *ExoIII* binds to the dsDNA. (2) *ExoIII* then selectively hydrolyzes the probe DNA strand from the duplex, releasing the target DNA strand back into solution. (3) The released target DNA is then free to bind to another surface-bound ssDNA probe. This cyclic reaction will repeat until all ssDNA probes on the surface are destroyed by *ExoIII*.

amplification reaction scheme is possible utilizing DNA microarrays where the probe single-stranded DNA (ssDNA) is covalently attached to the surface via its 5'-end. Figure 1 shows an overview of the *ExoIII* surface enzymatic amplification process. This amplification process is analogous to recently described work performed in our research group using RNase H on RNA microarrays.^{16,17} An ssDNA microarray is fabricated via 5'-end immobilization creating 3'-terminated ssDNA array elements that are exposed to a solution containing both complementary DNA and *ExoIII*. The complementary target DNA will first hybridize to the probe on the surface forming a DNA duplex to which *ExoIII* will then bind (step 1). *ExoIII* selectively hydrolyzes the 3'-terminated probe and releases the target DNA back into solution (step 2). The released DNA can then hybridize to another DNA probe on the surface, leading to removal of another probe (step 3). This cyclic reaction allows a very small number of target DNA molecules to initiate the destruction of many DNA probes on the surface. The negative change in percent reflectivity due to probe loss can be easily measured, resulting in an amplified SPR imaging signal that is considerably larger than the smaller positive signal observed from direct hybridization adsorption.

EXPERIMENTAL SECTION

Materials. *ExoIII* (Promega; 1 unit/mL = 0.17 nM), 11-mercaptopundecylamine (MUAM; Dojindo), 9-fluorenylmethoxycarbonyl-*N*-hydroxysuccinimide (Fmoc-NHS; Novabiochem), sulfo-succinimidyl 4-(*N*-maleimidomethyl)cyclohexane-1-carboxylate (SSMCC; Pierce), and *N*-hydroxysuccinimidyl ester of methoxy-poly(ethylene glycol) propionic acid (PEG-NHS; Nektar; MW 2000) were all used as received. Tris buffer (pH 7.9) containing 50 mM Tris-HCl, 10 mM MgCl₂, and 250 mM KCl was used for

all reported hybridization and *ExoIII* digestion experiments. All of the 3'- and 5'-thiol-modified DNA oligonucleotides were obtained commercially from Integrated DNA Technologies (IDT) and were deprotected and purified using binary reversed-phase HPLC. The complementary DNA (HPLC purified) was also purchased from IDT. The thiol-modified DNA oligonucleotides used in these experiments are as follows: D₁ = 5' S-S(T)₁₅GTGTTAGCCTCAAGTG, D₂ = 5' S-S(T)₁₅GTCTATGCGTGAAGTG, D₃ = 5' S-S(CH₂)₆T₂₀, A₁ = 3' S-S(T)₁₅GTGAAGTCCGATTGTG, A₂ = 3' S-S(T)₁₅GTCAAGTGCATATCTG, and A₃ = 3' S-S(CH₂)₆T₂₀. The complementary DNA sequences used were as follows: C₁ = 5' CAC TTG AGG CTAACAC, which is the complementary sequence of both D₁ and A₁, and C₂ = 5' CAGTTCACGCATAGAC, which is the complementary sequence of D₂ and A₂. Note that D₁ and A₁ are the same sequences but differ by thiol modification of either the 3'- or 5'-ends. This also applies to D₂ and A₂ as well as D₃ and A₃. D₁ and D₂ are designed to not interact with each other and not form hairpin structures. The (T)₁₅ spacer improves the accessibility of the surface-bound DNA to both the target DNA and *ExoIII*. All rinsing steps were performed with absolute ethanol and Millipore filtered water. All the experiments were performed at 37 °C.

DNA Array Fabrication. A multistep chemical modification process developed previously was used to create ssDNA microarrays for SPR imaging experiments.²⁴ Briefly, a thin gold film (45 nm) was vapor deposited onto an SF10 glass slide (Schott Glass) with an underlayer of chromium (1 nm) using a Denton DV-502A metal evaporator. The gold slides (18 mm × 18 mm) were immersed in 1 mM ethanolic solutions of MUAM for at least 4 h. The amine terminal group of the self-assembled alkanethiol MUAM monolayer was then reacted with the hydrophobic protecting group Fmoc-NHS. By exposing the gold surface to UV radiation through a quartz mask containing patterns of 500 μm × 500 μm square features, patterns of bare gold square patches surrounded by the hydrophobic background were created. The slide was then immersed in MUAM for a further 2 h, and the resulting MUAM patches were reacted with the heterobifunctional cross-linker SSMCC to form a thiol-reactive maleimide-terminated surface. Thiol-modified sequences of DNA were then spotted onto the SSMCC array elements using a manually controlled pneumatic picopump. The Fmoc background was removed, and the regenerated MUAM background was reacted with PEG to prevent any nonspecific adsorption of target biomolecules. The surface coverage of the ssDNA monolayer was estimated to be ~5 × 10¹² molecules/cm². The DNA arrays fabricated in this manner demonstrated excellent reproducibility with a chip-to-chip variation of ~5% for repeated SPR imaging measurements of hybridization and *ExoIII* digestion.

Kinetic Flow Cell Design. A serpentine PDMS microfluidics system was used to continuously deliver small volumes of samples across the DNA microarray surface for kinetics measurements.^{25,26} Briefly, a PDMS microchannel featuring a serpentine pattern (670-μm width, 9.5-cm length, 200-μm depth, total volume ~10 μL) was

(24) Brockman, J. M.; Frutos, A. G.; Corn, R. M. *J. Am. Chem. Soc.* **1999**, *121*, 8044–8051.

(25) Wegner, G. J.; Wark, A. W.; Lee, H. J.; Codner, E.; Saeki, T.; Fang, S.; Corn, R. M. *Anal. Chem.* **2004**, *76*, 5677–5684.

(26) Lee, H. J.; Wark, A. W.; Goodrich, T. T.; Fang, S.; Corn, R. M. *Langmuir* **2005**, *21*, 4050–4057.

first treated with oxygen plasma for 10 s to enhance the hydrophilicity of the channel, which can in turn help the flow of aqueous samples inside the channel and also minimize any sample adsorption onto the walls of the channels. The microchannel/gold chip/prism assembly was then encased in a specially designed water-jacketed cell allowing the system temperature to be controlled to within 0.1 °C. As a result, any fluctuations in SPR signal over time owing to room-temperature variations are also reduced. A syringe pump at a constant flow rate of 30 $\mu\text{L}/\text{min}$ was used to deliver all solutions through the microchannel.

Real-Time SPR Imaging Measurements. An SPR imaging apparatus (GWC Technologies) was used for the real-time monitoring of the DNA hybridization and *ExoIII* reaction. Briefly, collimated p-polarized light is reflected through a microchannel/gold chip/prism assembly at a fixed angle and then passed through a narrow band-pass filter and sent to a CCD camera. The image and kinetic data were collected using the software package V++ (Digital Optics, NZ). Custom macros were written using this software so that data could be collected with simultaneous processing of several specific user-designated regions of interest (ROIs) on the array surface.²⁵ For real-time measurements, a five-frame averaged image was saved and analyzed with the calculated change in average pixel intensity resulting in a data point collected for each ROI. During hybridization experiments, a time interval of 10 s was typically set between data point acquisitions, whereas for the *ExoIII* reaction, a 2-s time interval was applied. The difference in percent reflectivity ($\Delta\%R$) for each array element was normalized with respect to the average $\Delta\%R$ measured for the negative control and PEG background ROIs. Kinetic data from multiple identical array elements were averaged to obtain the final SPR response curve. Microsoft Excel and Igor Pro were used for all data processing and kinetic model fitting in these experiments.

RESULTS AND DISCUSSION

(A) Exonuclease III Reactivity with 5'- and 3'-Terminated DNA Microarrays. Our first task is to verify and quantitate the reactivity of *ExoIII* with the surface-bound DNA arrays. *ExoIII* is known to have 3'- to 5'-exonuclease activity for dsDNA in solution.^{26–28} Single-stranded DNA arrays were fabricated by covalently attaching thiol-modified oligos to a maleimide-terminated alkanethiol monolayer via either the 3'- or 5'-end²⁴ as shown schematically in Figure 2. For the case of 3'-end attachment (scheme a), the ssDNA array element is 5'-terminated. Hybridization with a complementary DNA oligomer from solution will result in a dsDNA array, and the 3'-terminated target DNA strand from the duplex will be digested by *ExoIII*; only the complementary DNA strand will be destroyed, leaving the original ssDNA still attached to the surface. In contrast, when the ssDNA array element is attached via the 5'-end, creating a 3'-terminated ssDNA element (scheme b in Figure 2), the exonuclease activity of *ExoIII* should result in the destruction of the surface-attached ssDNA and the release of the complementary DNA back into solution.

A series of real-time SPR imaging measurements were performed to verify the directional behavior of the surface *ExoIII* reaction with dsDNA. Two three-component ssDNA arrays were constructed using either 5'-terminated (scheme a) or 3'-terminated

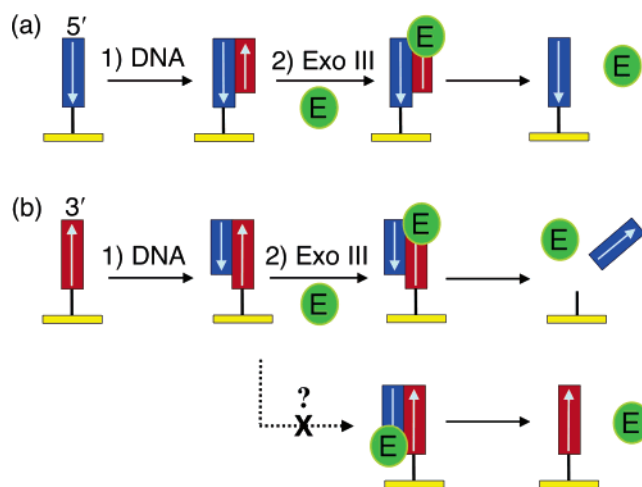


Figure 2. Schematic representation of the 3'- to 5'-exonuclease activity of *ExoIII* with (a) 5'- and (b) 3'-terminated ssDNA microarrays. (1) The ssDNA arrays are fabricated by attaching either (a) 3'- or (b) 5'-thiol-modified ssDNA to a maleimide-terminated alkanethiol monolayer. dsDNA arrays are then formed by hybridization of a complementary DNA oligomer from solution to the ssDNA. (2) Upon exposure of the dsDNA array to *ExoIII*, the enzyme selectively digests only (a) the target DNA where the probe DNA is 5'-terminated or (b) the probe DNA where it is 3'-terminated, by sequentially releasing 5'-mononucleotides into the bulk solution.

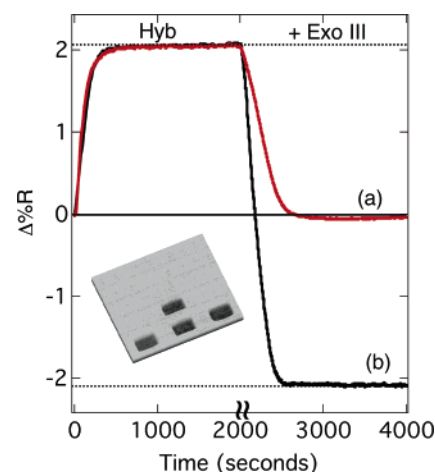


Figure 3. Real-time SPR imaging curves showing the sequence-specific hybridization adsorption of a 100 nM solution of the complementary DNA C_1 onto (a) 5'- and (b) 3'-terminated ssDNA array elements followed by the hydrolysis of dsDNA microarrays at an *ExoIII* concentration of 80 nM at 37 °C. The 5'-terminated ssDNA array in (a) is composed of A_1 , A_2 , and A_3 , and the 3'-terminated ssDNA array in (b) consists of D_1 , D_2 , and D_3 . C_1 is the complementary sequence of both A_1 and D_1 , which is designed to not interact with any of the other array components. The figure inset is a representative SPR difference image obtained by subtracting images acquired before and after *ExoIII* hydrolysis of dsDNA (D_1-C_1) array elements. The array element pattern is shown in Figure 5c.

ssDNA (scheme b) monolayers. The surfaces were then exposed to a 100 nM solution of the 16-mer complement of one of the three DNA sequences (C_1), and the resultant change in percent reflectivity ($\Delta\%R$) was measured as a function of time. Figure 3 plots these data and shows that a rapid rise in $\Delta\%R$ was observed at the appropriate ssDNA elements due to hybridization adsorption of the complement onto the surface, reaching a steady-state $\Delta\%R$ value of +2% after ~ 250 s. Both the 3'-terminated and 5'-terminated

(27) Hoheisel, J. D. *Anal. Biochem.* **1993**, *209*, 238–246.

(28) Weiss, B. In *The enzymes*; 3rd ed.; Boyer, P. B., Ed.; Academic Press, Inc.: New York, 1981; Vol. 14, pp 203–231.

ssDNA monolayers exhibited very similar hybridization adsorption kinetics. Not shown in Figure 3 are the $\Delta\%R$ curves obtained at the array elements containing the two noncomplementary DNA array sequences; these are used as controls for nonspecific adsorption and showed no change in $\Delta\%R$ during the experiment.

Following hybridization, the array was rinsed with buffer solution and then exposed to *ExoIII* (80 nM). For the case of the 5'-terminated array, exposure to the *ExoIII* solution resulted in a $\Delta\%R$ decrease of -2% back to the original reflectivity level (curve a in Figure 3). In contrast, for the case of the 3'-terminated array, a decrease of -4% was observed corresponding to the loss of both the target and probe DNA from the surface (curve b and see also Figure 3 inset). This is exactly what we expected to see for our two reaction schemes in Figure 2. As additional confirmation, we were able to reabsorb complementary 16-mer ssDNA onto the 5'-terminated ssDNA monolayer and observe a $\Delta\%R$ of $+2\%$, but no reabsorption or change in $\Delta\%R$ was observed for the 3'-terminated ssDNA monolayer.

These experiments allow us to draw the following conclusions about the *ExoIII* surface enzymatic reaction: (i) with either 5'-terminated or 3'-terminated ssDNA monolayers, *ExoIII* can completely digest the dsDNA monolayer formed by hybridization adsorption; (ii) for the case of the 3'-terminated ssDNA monolayer, the entire ssDNA can be removed by *ExoIII* digestion. This second point is important because, in principle, *ExoIII* could possibly digest the complementary strand as shown in the alternative reaction path of scheme b in Figure 2 (the reaction path containing a question mark). However, this would result in the incomplete digestion of the 3'-terminated ssDNA monolayer, which was not observed.

A final caveat to the use of *ExoIII* for the digestion of 3'-terminated DNA monolayers is that, on rare occasions, *ExoIII* activity was observed for ssDNA array elements without hybridization (data and sequences not shown). This unusual ssDNA activity was identified with sequences that formed hairpins on the surface, to which the enzyme was able to bind and interact. No *ExoIII* digestion of the 3'-terminated ssDNA array elements (D_1 , D_2 , D_3) reported in this paper was observed in the absence of duplex formation.

(B) Surface Amplification Process for DNA Detection.

Having characterized the reaction of *ExoIII* on 3'-terminated DNA monolayers, we are now in a position to use the enzyme amplification scheme depicted in Figure 1 for the detection of low concentrations of DNA target molecules. Before demonstrating the enzymatically amplified detection of DNA with *ExoIII*, we first wish to show the detection limit without amplification, i.e., SPR imaging measurements of direct DNA adsorption. The detection of DNA by hybridization adsorption with SPR and SPR imaging has been demonstrated previously by a number of research groups; for DNA monolayer adsorption, typically a detection limit in the range of 1–10 nM is reported.^{10,14,21–23,29–32} Figure 4 plots the SPR imaging response upon exposure of a ssDNA monolayer

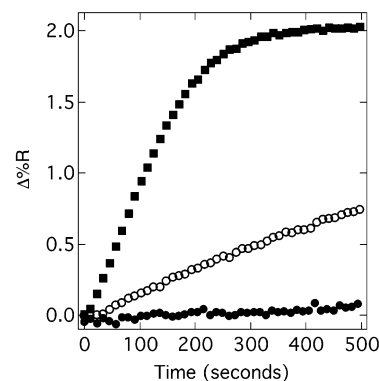


Figure 4. (a) Compiled real-time curves from SPR imaging measurements at various DNA concentrations for the sequence-specific hybridization adsorption of the DNA C_2 onto D_2 array elements at 37 °C. A three-component array such as the one in Figure 5c was used for the measurement. The three curves correspond to 1 (■), 10 (○), and 100 nM (●) C_2 . Each concentration curve was obtained by averaging the data set from five different arrays.

to 1, 10, and 100 nM solutions of complementary 16-mer DNA (C_2). Note that, at short times (<150 s), the adsorption kinetics are linear for all three concentrations. The adsorption rate, as determined from the initial slopes, decreases by factors of 10 as the target DNA concentration is reduced from 100 to 10 to 1 nM as expected from simple Langmuir kinetics. The slope of the 1 nM data is almost zero, and the SPR difference image shows virtually no change after 500 s. We have reported previously the detection limit of SPR imaging to be in the range of 1–10 nM.^{21,23} It is important to recount the reasons for this detection limit: (i) with SPR imaging, we can typically sense changes in DNA surface coverages (θ) down to $\sim 2\%$ of a monolayer, or $\sim 10^{11}$ molecules/cm²; (ii) the Langmuir adsorption coefficient K_{Ads} for 16-mer DNA hybridization adsorption is $\sim 2 \times 10^7$ M⁻¹, and since $\theta = K_{\text{Ads}} \cdot C$, 1 nM is the detection limit; and (iii) as seen in Figure 4, at low concentrations the adsorption kinetics become rather slow, so that competition with nonspecific adsorption becomes fairly significant, often limiting the detection of the specific hybridization adsorption of DNA. All of these points have also been noted by other researchers when discussing the detection limits of various SPR and other label-free DNA hybridization adsorption measurements.^{29,32–38}

As stated previously, we have recently employed RNA microarrays and the enzyme RNase H to increase the sensitivity of DNA detection with SPR imaging from 10 nM to 1 fM.^{16,17} Figure 5 shows our experiments using DNA microarrays and the enzyme *ExoIII* for enzymatically amplified SPR imaging using the reaction scheme in Figure 1. *ExoIII* and target DNA are simultaneously introduced into the microfluidic reaction channel containing the 3'-terminated ssDNA array elements. Adsorption of the target DNA onto the monolayer followed by *ExoIII* digestion results in

(29) Su, X.; Wu, Y.; Robelek, R.; Knoll, W. *Langmuir* **2005**, *21*, 348–353.
 (30) Mannella, I.; Minunna, M.; Tombellia, S.; Wanga, R.; Spiritia, M. M.; Mascinia, M. *Bioelectrochemistry* **2005**, *66*, 129–138.
 (31) Mark, S. S.; Sandhyarani, N.; Zhu, C.; Campagnolo, C.; Batt, C. A. *Langmuir* **2004**, *20*, 6808–6817.
 (32) Watts, H. J.; Yeung, D.; Parkes, H. *Anal. Chem.* **1995**, *67*, 4283–4289.

(33) Levicky, R.; Horgan, A. *Trends Biotechnol.* **2005**, *23*, 143–149.
 (34) Yu, F.; Yao, D.; Knoll, W. *Nucleic Acids Res.* **2004**, *32*, e75.
 (35) Peterson, A. W.; Heaton, R. J.; Georgiadis, R. M. *Nucleic Acids Res.* **2001**, *29*, 5163–5168.
 (36) Peterson, A. W.; Heaton, R. J.; Georgiadis, R. M. *J. Am. Chem. Soc.* **2000**, *122*, 7837–7838.
 (37) Steel, A. B.; Levicky, R. L.; Herne, T. M.; Tarlov, M. J. *Biophys. J.* **2000**, *79*, 975–981.
 (38) Liebermann, T.; Knoll, W.; Sluka, P.; Herrmann, R. *Colloids Surf., A* **2000**, *169*, 337–350.

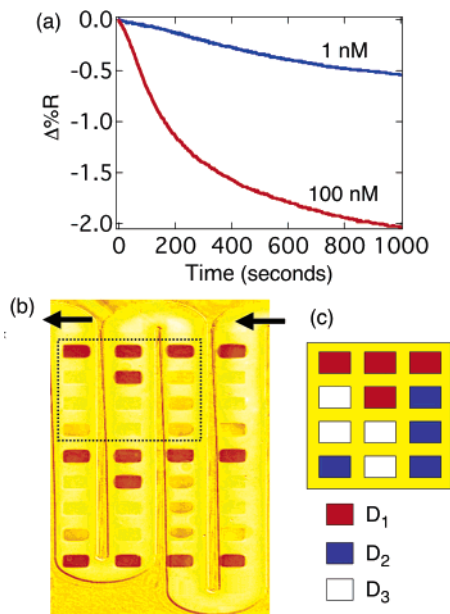


Figure 5. (a) Real-time SPR imaging curves obtained for the simultaneous hydrolysis of different dsDNA array elements by *ExoIII* when a solution containing a mixture of 80 nM *ExoIII*, 100 nM C₁, and 1 nM C₂ was introduced onto a three-component ssDNA array consisting of D₁, D₂, and D₃. The starting time of 0 s refers to when the ssDNA array surface was first exposed to the solution mixture. (b) An SPR difference image obtained by subtracting images taken before and after the ssDNA array has been exposed to the solution mixture for 60 min. The arrows represent the flow direction of the target DNA in the serpentine microchannel flow cell. (c) Schematic representation of the pattern of the three-component ssDNA array. Probes D₁ and D₂ are designed to bind to the target DNA C₁ and C₂, respectively, and probe sequence D₃ is a negative control. All experiments were carried out at 37 °C.

a decrease in $\Delta\%R$. In the experiment shown in Figure 5, two complements were introduced into the reaction channel with *ExoIII*: 100 nM complement DNA (C₁), and 1 nM complement DNA (C₂). D₃ is used as a control element. After 1000 s, the majority of the ssDNA has been removed from the D₁ array elements (as evidenced by the fact that the $\Delta\%R$ is $\sim -2\%$). A significant amount of the D₂ array elements has also been removed by the 1 nM C₂ and *ExoIII* solution corresponding to a $\Delta\%R$ of -0.5% ; this is clear evidence of the amplification process in which one complement can digest multiple ssDNA probe molecules.

Unfortunately, the amplification process is not as rapid as that observed for the case of RNase H and RNA microarrays.^{16,17} We attribute this slower reactivity to two possible causes: (i) *ExoIII*

is a processive enzyme as compared to RNase H, so the reaction rate is very slow at low DNA surface coverages, possibly leading to incomplete digestion of the ssDNA array elements, or (ii) perhaps at these very low surface coverages, the 3'-end of the hybridized target DNA is accessible to *ExoIII*, and adsorbed target molecules can be destroyed by the surface reaction marked with a question mark in Figure 2b. In any event, we find that enzymatic amplification can be achieved with *ExoIII* digestion, but only down to a new detection limit of 10–100 pM. This is still significantly lower than the 1–10 nM limit for DNA detection by hybridization adsorption without enzymatic amplification.

CONCLUSIONS

The ability to sensitively detect multiple DNA sequences simultaneously on a single chip without the use of labeling is of importance in many ongoing biosensing applications. Through the use of *ExoIII* in conjunction with DNA microarrays, a 10^2 – 10^3 improvement in the detection limit for the multiplexed SPR imaging detection of 16-mer oligonucleotides was achieved. This enhancement is not as great as RNase H amplification with RNA microarrays; however, the major advantage of *ExoIII* amplification compared to RNase H is that the additional difficulty in preparing and handling RNA microarrays is avoided. The *ExoIII* enzymatic amplification process can be used with the more robust and cost-effective DNA microarrays that are currently applied in research areas such as gene analysis and medical diagnostics. As in the case of RNase H amplification, most DNA sequences can be detected since the activity of *ExoIII* is not sequence dependent, although caution is required to avoid using probe DNA that may form hairpin structures resulting in signal loss without hybridization adsorption. Furthermore, this enzymatic amplification method can in principle be used in conjunction with other detection methods such as fluorescence and electrochemical measurements, as will be demonstrated in future papers.

ACKNOWLEDGMENT

This research is funded by the National Institute of Health (2R01 GM059622-04), the National Science Foundation (CHE-0133151), and a startup grant from the University of California, Irvine. The authors thank Shiping Fang for his insightful discussion concerning *ExoIII* activity.

Received for review May 11, 2005. Accepted June 3, 2005.

AC050815W